Probing the stability of gravastars by dropping dust shells onto them

Merse E Gáspár, István Rácz

Probing the stability of gravastars by dropping dust shells onto them

Merse E. Gáspár and István Rácz

RMKI, H-1121 Budapest, Konkoly Thege Miklós út 29-33. Hungary

E-mail: merse@rmki.kfki.hu, iracz@rmki.kfki.hu

Abstract. As a preparation for the dynamical investigations, this paper starts by providing a short review of the three-layer gravastar model with distinguished attention to the structure of the pertinent parameter space of gravastars in equilibrium. Then the radial stability of these type of gravastars is studied by determining their response for the totally inelastic collision of their surface layer with a dust shell. It is assumed that dominant energy condition holds and the speed of sound do not exceed that of the light in the matter of the surface layer. While in the analytic setup the equation of state is kept to be generic, in the numerical investigations three functionally distinct class of equation of states are applied. In the corresponding particular cases the maximal mass of the dust shell that may fall onto a gravastar without converting it into a black hole is determined. For those configurations which remain stable the excursion of their radius is assigned. It is found that even the most compact gravastars cannot get beyond the lower limit of the size of conventional stars, provided that the dominant energy condition holds in both cases. It is also shown—independent of any assumption concerning the matter interbridging the internal de Sitter and the external Schwarzschild regions—that the better is a gravastar in mimicing a black hole the easier is to get the system formed by a dust shell and the gravastar beyond itsthe event horizon of the composite system. In addition, a generic description of the totally inelastic collision of spherical shells in spherically symmetric spacetimes is also provided in the appendix.

PACS numbers: 04.40.Dg, 97.60.Lf, 04.20.Jb, 95.36.+x

Submitted to: *Class. Quantum Grav.*

1. Introduction

There are more and more astrophysical observations justifying the existence of extremely compact massive objects with size close to their Schwarzschild radius [1, 2, 3]. It is widely held that these observations do also provide indirect justifications of the existence of black holes (BHs). Nevertheless, there are also alternative ideas around claiming that exotic states of matter may exist which could stabilize extremely compact stars suiting to the aforementioned astrophysical observations (see, e.g., [4] for a recent review). One of

the most popular among these type of BH mimicing objects is the gravitational vacuum star (gravastar) model which has received considerable attention not least because its relation to the concept of dark energy. In this model of Mazur and Mottola [5] an interior de Sitter spacetime region is connected via three intermediate layers to an outer Schwarzschild solution such that the radius of the outermost layer is supposed to be slightly larger than the Schwarzschild radius of the system.

It is worth mentioning that in advance to the gravastar model there were several constructions in which the matching of a de Sitter region to the Schwarzschild spacetime was applied. For instance, to get read of the $r = 0$ singularity of the Schwarzschild spacetime Frolov, Markov and Mukhanov in [6] proposed a matching of a de Sitter interior to it at a small radius of Planck scale ensuring thereby that the curvature remains bounded everywhere in the yielded spacetime. Dynamical investigation of this model was already carried out in [7].

Note that up to certain extent the model used in [6] could be considered as the precursor of the gravastar model—although in the latter the matching was made in a more elaborated way—and the outermost matching surface, at the boundary of the Schwarzschild region, was supposed to be arranged such that its radius is slightly larger than the pertinent Schwarzschild radius.

Once such a model is set up the following questions manifest themselves:

(1) What type of physical process may produce such a gravastar?

(2) Is a gravastar stable?

(3) If it is, does it provide a viable alternative to BHs?

While the first question has not been tackled yet even the second question turned to be too complex within the original model of Mazur and Mottola—although in [5] an argument claiming for the thermodynamical stability of it was given—as it is composed by making use of three different types of regions with unspecified matter. To reduce the related ambiguities Visser and Wiltshire [8] introduced a simplified three-layer gravastar model where the interior de Sitter region is matched to the exterior Schwarzschild spacetime via a single matter shell. This model is simple enough to carry out various analytic investigations by making use of the thin-shell formalism of Israel [9]. Visser and Wiltshire besides deriving the basic relations determining the evolution of gravastars did also carried out the first investigation of their radial stability. Since then the stability of gravastars has been studied by several authors within this simplified model or within its continuum correspondence [10]. Results relevant for radial stability may be found in [11, 12], and in case of electrically charged gravastars in [13]. The stability has also been investigated with respect to axial perturbations [14, 15].

In all of these investigations attention was restricted to the space of gravastars in equilibrium, i.e., the radial stability was investigated by determining the response of a gravastar to a slight formal change of the underlying effective potential. For instance, in [16, 17] the excursions of gravastars was investigated this way such that their evolution started with carefully prepared initial conditions. In all of the pertinent investigations it

was demonstrated that by suitably adjusting the equation of state (EOS) of the matter forming the surface of the gravastar the subspace of "stable" gravastars may always be ensured to be of non-zero measure. Nevertheless, it was also found that whenever the measure of the subspaces of the configuration space representing stable and unstable gravastars are compared the former is always found to be negligible with respect to the latter. This observation was commonly interpreted that gravastars may not offer a viable alternative to BHs.

The main purpose of the present paper is to determine the response of a gravastar in equilibrium to the arrival of a dust shell onto its surface. This is done—not merely by considering some formal change of the effective potential determining the state of a gravastar—but by making use of the full dynamical setup. For the sake of definiteness, we assume that the surface of the gravastar and the dust shell collide in a totally inelastic manner. In addition, concrete EOSs are chosen and it is assumed that the dominant energy condition (DEC) holds‡ and the speed of sound in the surface of the gravastar does not excide that of the light. Then the relevant non-linear problem—the basic equations of which are based on the generic dynamics of spherical shells—are solved by using analytic and numerical approaches. In this way not only the excursion of particular gravastar models may be studied but we could determine the maximal mass of the dust shell colliding with the surface of the gravastar without converting the latter into a BH.

This paper is organized as follows. In Section 2 some of the basics of the Visser and Wiltshire three-layer dynamics gravastar model are recalled using dimensionless variables. As a byproduct of our preparation for the aforementioned dynamical investigations a short survey of the configuration space of stable gravastars is also provided . (Although there are no completely new results in this section we believe that this review provides a good reference frame for the results of the succeeding dynamical investigations.) In Section 3 the dynamics of the system composed by the spherically symmetric dust shell falling onto a stable gravastar, along with their collision, is described. Section 4 is to report about our analytic and numerical results concerning the dynamics of maximally loaded gravastars, while Section 5 contains the finalour concluding remarks. Finally, in the appendix, a generic description of the totally inelastic collision of spherical shells in spherically symmetric spacetimes is also provided. Throughout this paper the geometrized units, with $G = c = 1$, are applied.

2. Gravastar model of Visser and Wiltshire

Throughout this paper considerations will be restricted to the three-layer spherically symmetric gravastar model of Visser and Wiltshire [8]. This simplified model consists of an external Schwarzschild vacuum region with mass parameter M—representing the

‡ Recall that the dominant energy condition guarantees that the concept of causality is properly adopted in general relativity. Therefore, the exclusion of matter models yielding its violation seems to be preferable.

total ADM mass of the gravastar—, an interior de Sitter region with energy density, ρ_0, and an infinitesimally thin shell at the mutual boundary of the aforementioned two regions at radius a with surface energy density σ and surface tension θ. The line element representing the interior de Sitter and exterior Schwarzschild spacetimes is given in the appendix by (A.1) and (A.2), where the pertinent forms of $M_K(r)$ are specified in the paragraph below (A.2). Note that the radius is allowed to vary in time. As the shell is assumed to coincide, at any moment, with one of the $SO(3)$ group orbits the quantities characterizing the shell are functions only of the radius. To have a closed system of equations governing the evolution of the shell we also need to assume the existence of an EOS. As it was noted above σ and θ must be functions of the radius exclusively. Thereby, in virtue of the implicit function theorem, the EOS, relating the tension, θ, of the surface to the mass density, σ, of the surface of the gravastar, may always be assumed to possess the form $\theta = \theta(\sigma)$. This section is, beside recalling the most important equations determining the dynamics, is also to provide a short comprehensive review of the basic properties of the above outlined three-layer gravastar model.

2.1. Parametrization

In studying the gravastar model the use of the following dimensionless parameters turned out to be advantageous. They are the dimensionless radius $\alpha = a/(2M)$, surface density $\Sigma = \sigma M$, tension $\Theta = \theta M$, and the dimensionless de Sitter density parameter, $\eta = 8kM^2$, where $k = 4\pi\rho_0/3$.§ Note that in the chosen setup positive tangential pressure does correspond to negative surface tension. To avoid the appearance of the event horizon in the Schwarzschild region the inequality $1 < \alpha$ is required to be satisfied. Similarly, in order to exclude the presence of a "cosmological" horizon in the de Sitter region the inequality $\alpha < \eta^{-1/2}$ is imposed. Accordingly, in case of the considered gravastar models the value of η is restricted to the interval $0 < \eta < 1$. Note finally, that in dynamical situations the time dependence may conveniently be expressed via the dimensionless proper time, measured, by observers moving radially along the world-sheet of the shell, in $2M$ units.

2.2. Dynamical equations

The basic equations determining the dynamics of the shell of the gravastar can be derived in various ways. The most widely applied method uses the thin-shell formalism of Israel [9] based on the results of Sen, Lanczos, Darmois [18, 19, 20]. In this approach the induced metrics, h^-_{AB} and h^+_{AB}, on the mutual boundary of the two spacetime regions—the inner and the outer—on the two sides of the shell are assumed to coincide, i.e., the metric on the shell can be given as $h_{AB} = h^+_{AB} = h^-_{AB}$, while the discontinuity of the pertinent extrinsic curvature tensors, K^+_{AB} and K^-_{AB}, are related to the surface-energy

§ Whenever $\eta = k = 0$ the systems degenerates to a shell moving in a Minkowski-Schwarzschild spacetime.

density $S_{AB} = \mathrm{diag}(\sigma, -\theta, -\theta)$ via the matching condition‖

$$K^{+}_{AB} - K^{-}_{AB} = -8\pi \left\{ S_{AB} - h_{AB}(h^{CD} S_{CD}) \right\} . \tag{2.1}$$

By making use of the pertinent results of [8], along with the above introduced parameterization, these junction conditions can be seen to take the form

$$\Sigma = \frac{1}{8\pi\alpha} \left(\sqrt{1 - \eta\alpha^2 + \dot{\alpha}^2} - \sqrt{1 - \alpha^{-1} + \dot{\alpha}^2} \right) , \tag{2.2}$$

$$\Theta = \frac{1}{16\pi\alpha} \left(\frac{1 - 2\eta\alpha^2 + \dot{\alpha}^2 + \alpha\ddot{\alpha}}{\sqrt{1 - \eta\alpha^2 + \dot{\alpha}^2}} - \frac{1 - \alpha^{-1}/2 + \dot{\alpha}^2 + \alpha\ddot{\alpha}}{\sqrt{1 - \alpha^{-1} + \dot{\alpha}^2}} \right) . \tag{2.3}$$

where the over-dot denotes the derivative with respect to the dimensionless proper time along the shell.

As the energy density of the shell is always assumed to be non-negative the first square root on the left hand side of (2.2) must be greater than the second one, which implies that $\alpha < \eta^{-1/3}$. Note that this restriction, viewed as a condition on the value of α, is more demanding than the previous one excluding the presence of a cosmological horizon in the inner de Sitter region. In virtue of (2.2) it is straightforward to see that whenever Σ is non-negative it attains its maximum value for vanishing $\dot{\alpha}$ for any fixed value of α.

In describing the dynamics of gravastars it turned out to be advantageous to introduce an "effective potential" defined via the relation

$$V(\alpha; \eta) = -\frac{\dot{\alpha}^2}{2} . \tag{2.4}$$

Assuming that Σ is positive, by a straightforward algebraic manipulation, one gets that V can be given as a function of α and $\Sigma = \Sigma(\alpha)$—it also depends on the dimensionless de Sitter density parameter η—and it reads as

$$V(\alpha, \Sigma(\alpha); \eta) = \frac{1}{2} \left[1 + \frac{\eta}{64\pi^2 \alpha\, \Sigma^2(\alpha)} - \left(4\pi\alpha\, \Sigma(\alpha) + \frac{1 + \eta\alpha^3}{16\pi\alpha^2\, \Sigma(\alpha)} \right)^2 \right] , \tag{2.5}$$

which, in virtue of (2.4)—despite of its complicated analytic form— has to be smaller than or equal to zero.

Once Σ is known as a function of the dimensionless radius, α, so is $V(\alpha; \eta)$, and, in turn, (2.4) can be used to determine the motion of the shell. The next subsection is to show that the EOS of the shell, along with the conservation law, $D^A S_{AB} = 0$—where D_A denotes the covariant derivative operator compatible with the metric, h_{AB}, on the shell—can be used to determine the functional form of $\Sigma(\alpha)$.

‖ This relation corresponds essentially to the Lanczos equation.

2.3. Equation of state of the shell

Recall first that the EOS of the surface matter of the gravastar, if given in terms of the dimensionless variables, may be assumed to possess the form $\Theta = \Theta(\Sigma)$. Admittedly, the entire concept of an infinitesimally thin shell may be considered to be somewhat artificial. Nevertheless, in our investigations we need to apply some assumptions on the type of its matter. The use of a suitable energy condition is essential. In this respect the use of the DEC seems to be the most appropriate which is knownsupposed to guarantee that the concept of causality is properly adopted in describing the evolution of coupled gravity matter systems. Note that the less stringent weak and null energy conditions are automatically satisfied whenever DEC is guaranteed to hold. For an infinitesimally thin shell DEC can be seen to hold whenever $|\Theta| < \Sigma$ [21].

Throughout this paper the function $\Theta = \Theta(\Sigma)$ will be assumed to be continuous and piecewise differentiable. To avoid dynamical instabilities we shall also assume that the square of the speed of sound, $c_{\rm s}^2 = -{\rm d}\Theta/{\rm d}\Sigma$, is non-negative, and to be compatible with the concept of relativity that $c_{\rm s}^2$ is required to be less than or equal to the square of the speed of light. Accordingly, unless otherwise stated, it will be assumed that $0 \leq c_{\rm s}^2 \leq 1$.

It is well-known that the radial conservation equation

$$\frac{\rm d}{{\rm d}\tau}\left(\Sigma\alpha^2\right) = \Theta\frac{\rm d}{{\rm d}\tau}\left(\alpha^2\right)\,, \tag{2.6}$$

where τ denotes the dimensionless proper time along the radial trajectories generating the shell. (2.6) may be derived either by referring to the conservation law $D^A S_{AB} = 0$ or by making use of equations (2.2) and (2.3) as in [8]. By introducing the dimensionless radius α, instead of τ, as an independent variable (2.6) takes the form

$$\alpha\frac{{\rm d}\Sigma}{{\rm d}\alpha} = 2(\Theta - \Sigma)\,. \tag{2.7}$$

This is the very point where the EOS of the shell comes into play since by substituting the relation $\Theta = \Theta(\Sigma)$ into (2.7) the functional form of $\Sigma = \Sigma(\alpha)$ can be determined. Note that as $\Theta - \Sigma < 0$, in virtue of (2.7), $\Sigma(\alpha)$ has to be a monotonic decreasing function, and also as (2.7) is a separable differential equation an implicit solution of it can be given as

$$\frac{\alpha}{\alpha_0} = \exp\left(\frac{1}{2}\int_{\Sigma_0}^{\Sigma(\alpha)}\frac{{\rm d}\widetilde{\Sigma}}{\Theta(\widetilde{\Sigma}) - \widetilde{\Sigma}}\right), \tag{2.8}$$

where the integration constant Σ_0 is fixed such that $\Sigma_0 = \Sigma(\alpha_0)$.¶

To have some specific examples in latter sections we shall use the following three types of EOS. The simplest EOS—that have been used in most of the former investigations of gravastars—is linear homogeneous possessing the functional form

$\Theta(\Sigma) = -w_0\,\Sigma$, which, however, is not satisfied for a generic linear functional relation. In this case $c_{\rm s}^2 = w_0$ and

$$\Sigma(\alpha) = \Sigma_0 \left(\frac{\alpha}{\alpha_0}\right)^{-2(1+w_0)} . \tag{2.9}$$

Clearly, it is of interest to consider more complex systems, as well. Since $\mathrm{d}\Theta/\mathrm{d}\Sigma$ is related to the speed of sound and its value at an equilibrium point will play an important role in the stability of the gravastar it seems to be reasonable consider EOSs with varying sound speed at the equilibrium point. The simplest generalization of homogeneous linear EOS would be the non-homogeneous linear one. However, we would also like to have DEC to hold which requires Θ to vanish at $\Sigma = 0$. Therefore we use instead the "broken linear" EOS

$$\Theta(\Sigma) = \begin{cases} -w_1\Sigma & , \text{if } \Sigma \le \Sigma_1 \\ -w_1\Sigma_1 - w_2(\Sigma - \Sigma_1) & , \text{if } \Sigma > \Sigma_1 . \end{cases} \tag{2.10}$$

Here the parameter Σ_1 signifies the value of the breaking point in the Σ range, while for the values of the slopes, w_1 and w_2, before and after the matching the inequalities $0 \le w_1, w_2 < 1$ hold. Then (2.8) can be evaluated explicitly. In doing so the dimensionless radius of the matching point α_1, gets to be determined by the relation $\Sigma_1 = \Sigma(\alpha_1)$ as

$$\alpha_1 = \begin{cases} \alpha_0 \left(\frac{\Sigma_0}{\Sigma_1}\right)^{1/(2w_1+2)} & , \text{if } \Sigma_0 \le \Sigma_1 \\ \alpha_0 \left(\frac{\Sigma_0(1+w_2)+\Sigma_1(w_1-w_2)}{\Sigma_1(1+w_1)}\right)^{1/(2w_2+2)} & , \text{if } \Sigma_0 > \Sigma_1 . \end{cases} \tag{2.11}$$

Then, whenever $\Sigma_0 \le \Sigma_1$

$$\Sigma(\alpha) = \begin{cases} \Sigma_1 \frac{w_2 - w_1 + (1+w_1)\left(\frac{\alpha_1}{\alpha}\right)^{2w_2+2}}{1+w_2} & , \text{if } \alpha \le \alpha_1 \\ \Sigma_0 \left(\frac{\alpha_0}{\alpha}\right)^{2w_1+2} & , \text{if } \alpha > \alpha_1 , \end{cases} \tag{2.12}$$

while for $\Sigma_0 > \Sigma_1$

$$\Sigma(\alpha) = \begin{cases} \frac{\Sigma_1(w_2-w_1)+(\Sigma_0(1+w_2)+\Sigma_1(w_1-w_2))\left(\frac{\alpha_0}{\alpha}\right)^{2w_2+2}}{1+w_1} & , \text{if } \alpha \le \alpha_1 \\ \Sigma_1 \left(\frac{\alpha_1}{\alpha}\right)^{2w_1+2} & , \text{if } \alpha > \alpha_1 . \end{cases} \tag{2.13}$$

Another obvious choice is a polytrop EOS. Note, however, that in general a polytrop EOS is supposed to relate the rest energy density ε, as opposed to the total energy density σ, to the pressure in which case it takes the functional form $p = A\,\varepsilon^\kappa$, with parameters A and κ. Thereby, whenever we replace ε by σ the "inverse form" of the polytrop EOS reads as (see, e.g., [22])

$$\Sigma(\Theta) = \left(-\frac{\Theta}{A}\right)^{1/\kappa} - \frac{\Theta}{\kappa - 1} . \tag{2.14}$$

¶ Throughout this subsection the integration constant are determined by referring to certain α_0 value. Although latter α_0 will label equilibrium states it should keep in mind that α_0 does not have such an interpretation yet.

The solution of (2.8) can then be given explicitly as

$$\Sigma(\alpha)=\left(-\frac{\Theta_0}{A}\right)^{1/\kappa}\left(\frac{\alpha_0}{\alpha}\right)^2-\frac{\Theta_0}{\kappa-1}\left(\frac{\alpha_0}{\alpha}\right)^{2\kappa}, \tag{2.15}$$

where Θ_0 is related to the value of Σ_0 by (2.14).

It is straightforward to check that DEC satisfied if and only if $\kappa\in(1,2]$. Assume, now that we are given both of the values Σ_0 and Θ_0 and the EOS is chosen to possess the form (2.14) then κ has to take value from the interval $[1+w_0,2]$, where $w_0=-\Theta_0/\Sigma_0$. Then the square of initial speed of sound at Σ_0 can be given as $c_{\mathrm{s}}^2|_{\Sigma_0}=\kappa w_0/(1+w_0)$.

In closing this subsection let us emphasize again that whenever an EOS, $\Theta=\Theta(\Sigma)$, is chosen Σ may be given as a function $\Sigma=\Sigma(\alpha)$ and, in virtue of (2.5), the effective potential can be given as an explicit function $V(\alpha;\eta)$ depending exclusively on the dimensionless radius, α, and the dimensionless de Sitter density parameter, η.

2.4. Gravastars in equilibrium

In this subsection considerations will be restricted to the case of gravastars in equilibrium. Equilibrium, as usual, signifies those configurations in rest for which forces are also balanced, i.e., $V(\alpha_0;\eta)=0$ and $V'(\alpha_0;\eta)=0$, where α_0 stands for the value of α in equilibrium, while prime, $'$, denotes derivative with respect to α. As it is expected the vanishing of V and V' is equivalent to the vanishing of $\dot\alpha$ and $\ddot\alpha$, which can be verified by making use of (2.4). For instance, the vanishing of $\dot\alpha$ immediately follows from (2.4). In verifying the vanishing of $\ddot\alpha$ substitute first $-2V(\alpha)$ for $\dot\alpha^2$ in (2.2) and derive the yielded expression with respect to α. This justifies that, on the one hand, $\mathrm{d}\Sigma/\mathrm{d}\alpha$ depends on η, α, $V(\alpha)$ and $V'(\alpha)$. On the other hand, in virtue of (2.7) we have that $\mathrm{d}\Sigma/\mathrm{d}\alpha=2(\Theta-\Sigma)/\alpha$, which along with (2.2) and (2.3), can be used to deduce the relation $\ddot\alpha=-V'(\alpha)$.

It worth to be mentioned here that some of the authors (see, e.g., [8]) refer to these configurations as "static gravastars". This terminology is, however, partly confusing because for a 'static gravastar' the radius should be time independent, i.e., τ-derivatives of α should vanish up to arbitrary order. As opposed to this the vanishing of $V(\alpha_0;\eta)$ and $V'(\alpha_0;\eta)$ implies merely the vanishing of $\dot\alpha$ and $\ddot\alpha$ whereas, in general, the higher order τ-derivatives are not guaranteed to vanish.

In the rest of this subsection we intend to provide a depicting of the configuration space of gravastars in equilibrium. In depicting of the configuration space of gravastars in equilibriumdoing so we shall apply the values $\Sigma_0=\Sigma(\alpha_0)$ and $\Theta_0=\Theta(\alpha_0)$, which, by making use of (2.2) and (2.3), along with the vanishing of $\dot\alpha$ and $\ddot\alpha$ at $\alpha=\alpha_0$, can be given as

$$\Sigma_0=\frac{1}{8\pi\alpha_0}\left(\sqrt{1-\eta\alpha_0^2}-\sqrt{1-\alpha_0^{-1}}\right) \tag{2.16}$$

and

$$\Theta_0=\frac{1}{16\pi\alpha_0}\left(\frac{1-2\eta\alpha_0^2}{\sqrt{1-\eta\alpha_0^2}}-\frac{1-\frac{1}{2}\alpha_0^{-1}}{\sqrt{1-\alpha_0^{-1}}}\right). \tag{2.17}$$

Using the algebraic equations of (2.16) and (2.17) and the condition that $\Sigma_0(\eta, \alpha_0) > 0$, it can be shown that for a gravastar in equilibrium the surface tension, $\Theta_0(\eta, \alpha_0)$, is always negative. This justifies then that no exotic matter (with negative pressure) is required to form the shell of a gravastar in equilibrium.

Note that whenever an EOS is given only one of the values of η and α_0 can be chosen freely because, in virtue of (2.16) and (2.17), $w_0 = -\Theta_0/\Sigma_0$ has to be consistent with the EOS. On the other hand whenever no definite choice is made for an EOS then the configuration space of gravastars in equilibrium may be parameterized by η and α_0. In this case the value of $w_0(\eta, \alpha_0)$ gets to be determined by relations (2.16) and (2.17).

In depicting the configuration space of gravastars in equilibrium it is useful to identify the region on the $\alpha_0 - \eta(\alpha_0, \eta)$ plain where DEC holds (see Fig. 2). In doing so recall first that, whenever Σ_0 is non-negative for a gravastar in equilibrium Θ_0 has to be negative. This immediately implies that DEC reduces to $0 \leq w_0 \leq 1$, furthermore the upper boundary of the subregion of the (α_0, η) plain where DEC is satisfied is signified by the $w_0 = 1$ curve. This curve—determined by the implicit relation $w_0(\eta, \alpha_0) = 1$—can be given as

$$\eta_{\rm max}^{\rm DEC}(\alpha_0) = \frac{60\alpha_0^2 - 36\alpha_0 - 25 + (5 - 6\alpha_0)\sqrt{100\alpha_0^2 - 124\alpha_0 + 25}}{128\,\alpha_0^3\,(\alpha_0 - 1)}\,, \quad (2.18)$$

which intersects the α_0-axis at the value $\alpha_0 = 25/24$ (see Fig. 2). Consequently, whenever DEC holds α_0 has to be greater than or equal to $25/24$. This value of the minimal radius immediately imposes a strict limit on the compactness, expressed by the $2m/r$ ratio, of a gravastars in equilibrium. It also follows from (2.18) that for small η the approximation $\eta_{\rm max}^{\rm DEC} \approx \frac{2}{5}\alpha_0^{-3}$ holds.

For comparison it is useful recall that the value of the ratio $2m/r$ is also restricted in case of conventional star models composed by matter satisfying DEC. In case of spherically symmetric static configurations under various assumptions concerning the energy density and pressure of the star the ratio $2m/r$ has been investigated. A comprehensive summary of the pertinent results can be found in [23]. It is shown there that if pressure is non-negative (although it may be anisotrop) and DEC holds, then the numerical value of the sharp upper bound for $2m/r$ is 0.963.[+] It is interesting that the corresponding upper bound for a gravastar in equilibrium is a little bit smaller $24/25 = 0.96$. One of the readings of this finding is that whenever DEC holds the radius of the most compressed gravastar in equilibrium is definitely larger than the radius of the most compressed conventional star. This indicates then that instead of asking whether these gravastars can be distinguished from BHs, by any sort of astrophysical observations, it is more appropriate to ask whether they can be distinguished from the most compact stars.

[+] This numerical value is claimed to be precise up to three digits in [23].

2.5. Stable equilibrium

In deciding whether a gravastars is in equilibrium there has been no need to choose a specific EOS. Nevertheless, whenever we want to study the radial stability of these configurations we shall need to know the EOS, at least, in a sufficiently small neighborhood of Σ_0 as merely the knowledge of Θ_0 and Σ_0 will not suffice then.

Before turning to the radial stability of gravastars there are some conceptual issues to be mentioned. In spite of the familiarity of the dynamical equation $\dot{\alpha}^2/2 + V(\alpha;\eta) = 0$ it is better not applying automatically the analogous one-dimensional classical mechanical arguments. The main reason is related to the fact that $V(\alpha;\eta)$ is not an external potential. In case of the classical mechanical problem the "total energy" need not to be zero so we may simply increase either the kinetic energy term or change the potential energy by moving out of our system from its equilibrium. In both cases, since the potential is supposed to be intact, the total energy is changed. As opposed to this in case of a gravastar if the initial velocity is changed the potential has to be changed also since the formal "total energy" needs to remain zero. The changing the initial velocity $\dot{\alpha}$ affects the initial surface energy density, Σ_0, therefore the solution $\Sigma(\alpha)$ of (2.8), and, in turn, $V(\alpha, \Sigma(\alpha);\eta)$ is also affected. This verifies that it is better to avoid thinking of $V(\alpha, \Sigma(\alpha);\eta)$ as an external potential.

In carrying out the radial stability of gravastars we shall assume that V smoothly depends on its indicated variables. This implies then that under a sufficiently small perturbations of a gravastar in equilibrium the sign of the second derivative, $V''(\alpha_0)$, will be intact. In particular, since the perturbation increases the kinetic term the potential has to become negative in a sufficiently small neighborhood of α_0 whence the yielded motion of the gravastar will be bounded if the value of $V''(\alpha_0)$ is guaranteed to be positive. Accordingly, a gravastar in equilibrium, with radius α_0, is considered to be stable if $V''(\alpha_0;\eta) > 0$.

As it was already mentioned, the vanishing of $V(\alpha_0)$ and $V'(\alpha_0)$—in the classical mechanical analogy—corresponds to vanishing speed, $\dot{\alpha} = 0$, and, in turn, that the forces are balanced. The equilibrium configurations can be classified according to the convex-concave character of the potential, i.e., it is reasonable to distinguish the following three categories:

(a) *Stable*: A gravastar in equilibrium is considered to be stable whenever small perturbations of the system yields small local oscillations around the equilibrium state. In this case the potential has to be a convex function near α_0. This may happen whenever $V''(\alpha_0) > 0$. (See, e.g., the transition from potential 1 to potential 2 on Fig. 1).

(b) *Locally unstable*: This occurs if the potential is concave (at least from one side) near α_0. This means that small perturbations may yield non-local motions. This locally unstable situation may happen, e.g, whenever $V''(\alpha_0) < 0$. (For an illustration see graph 3 on Fig. 1, where α_1 takes the role of α_0). If V'' is not continuous at α_0 but

have well-defined left and right hand sided limit values the equilibrium state will be called locally unstable if either of these limit values is negative.

The vanishing of $V''(\alpha_0)$ may also occur. In this case the sign of the least non-zero α-derivative of V determines the character of the potential. For instance, the graph of V may change its character from concave into convex or vice versa through an inflexion point whenever V''' is the first non-zero higher order derivative. This means that the equilibrium is locally unstable in one direction. However if the first non-zero α-derivative of V is V'''' then the graph of V may have local minimum or maximum in accordance with the sign of V''''.

(c) *Neutral*: It may also happen that the potential is identically zero, $V(\alpha) \equiv 0$, in the neighborhood of α_0. In this particular case the equilibrium is called neutral (throughout this neighborhood).

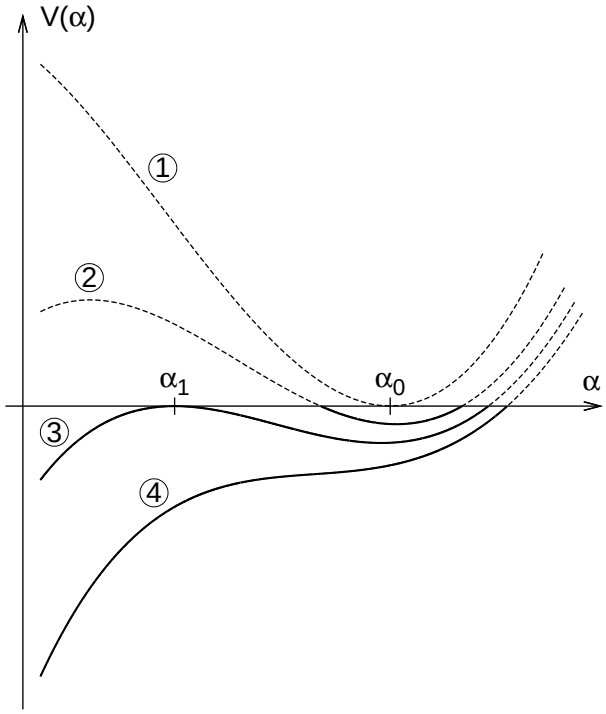

Figure 1. Typical potentials are indicated. The graph 1 depicts a potential relevant for stable equilibrium. The other three graphs, with label 2, 3 and 4, represent the change of the potential caused by dropping more and more massive spherical dust shells onto the same initially stable gravastar. In particular, graphs 2 and 3 comes with a bounded motion of the resulted gravastar, while in the case of graph 3 the exactly maximal mass was dropped onto the initially stable configuration. Graph 4 corresponds to the situation when the gravastar collapses to a BH.

In determining the value of $V''(\alpha_0)$ recall first that c_s^2 can be given as

$$c_s^2 = -\frac{\mathrm{d}\Theta}{\mathrm{d}\Sigma} = -\frac{\mathrm{d}\Theta/\mathrm{d}\alpha}{\mathrm{d}\Sigma/\mathrm{d}\alpha}\,. \tag{2.19}$$

The terms $\mathrm{d}\Theta/\mathrm{d}\alpha$ and $\mathrm{d}\Sigma/\mathrm{d}\alpha$ can be expressed by using equations (2.2) and (2.3). For instanceThen, in virtue of (2.5), and since $\dot{\alpha}^2 = -2V(\alpha)$ and $\ddot{\alpha} = -V'(\alpha)$, we find that

$\mathrm{d}\Sigma/\mathrm{d}\alpha$ can be given in terms of $V(\alpha)$ and $V'(\alpha)$ exclusively. Similarly, $\mathrm{d}\Theta/\mathrm{d}\alpha$ can be seen to depend on $V(\alpha)$, $V'(\alpha)$ and $V''(\alpha)$ exclusively, i.e., no higher order α-derivatives of $V(\alpha)$ are needed in evaluating $\mathrm{d}\Theta/\mathrm{d}\alpha$. Therefore, in case of a gravastar in equilibrium, i.e., whenever $V(\alpha_0) = 0$ and $V'(\alpha_0) = 0$, $V''(\alpha_0)$ can be expressed as a function of the variables η, α_0 and $c_{\mathrm{s}0}^2 = c_{\mathrm{s}}^2|_{\alpha_0}$. This means—as it was mentioned before—, in carrying out the stability analysis of gravastars in equilibrium only the derivative $\mathrm{d}\Theta/\mathrm{d}\Sigma = -c_{\mathrm{s}}^2$ of the EOS at Σ_0 comes into play.

It can be shown that fFor stable configurations $V''(\alpha_0)$ has to be positive which requires $c_s^2 > c_{s,\mathrm{min}}^2$ to hold, where the square of the speed of sound is bounded from below by

$$c_{s,\mathrm{min}}^2 = -\left.\frac{\partial\Theta/\partial\alpha}{\partial\Sigma/\partial\alpha}\right|_{\alpha_0} = -\frac{\partial\Theta_0/\partial\alpha_0}{\partial\Sigma_0/\partial\alpha_0}\,, \tag{2.20}$$

which is nothing but the square of the speed of sound $c_{\mathrm{s}0}^2$ at α_0 whenneverfor configurations with $V''(\alpha_0) = 0$.

To see that (2.20) holds note first that Σ and Θ—given originally as functions $\Sigma(\alpha, \dot\alpha; \eta)$ and $\Theta(\alpha, \dot\alpha, \ddot\alpha; \eta)$—in virtue of the relations $\dot\alpha^2 = -2V(\alpha;\eta)$ and $\ddot\alpha = -V'(\alpha;\eta)$ can be given as the functions of the form $\Sigma = \Sigma(\alpha, V(\alpha;\eta); \eta)$ and $\Theta = \Theta(\alpha, V(\alpha;\eta), V'(\alpha;\eta); \eta)$. Then (2.19), along with the relations $\mathrm{d}\Sigma/\mathrm{d}\alpha = \partial\Sigma/\partial\alpha + (\partial\Sigma/\partial V)\,V'$ and $\mathrm{d}\Theta/\mathrm{d}\alpha = \partial\Theta/\partial\alpha + (\partial\Theta/\partial V)\,V' + (\partial\Theta/\partial V')\,V''$, and the vanishing of $V'(\alpha;\eta)$ and $V''(\alpha;\eta)$ in case of a gravastar in equilibrium justifies the first equality in (2.20). The second one holds because, in virtue of (2.2) and (2.16) $(\partial\Sigma/\partial\alpha)|_{\alpha_0} = (\partial\Sigma_0/\partial\alpha_0)$, and similarly, in virtue of (2.3) and (2.17) $(\partial\Theta/\partial\alpha)|_{\alpha_0} = (\partial\Theta_0/\partial\alpha_0)$. Note also that by taking into account (2.16) and (2.17) the minimal value of $c_{\mathrm{s}0}^2$ can be given as

$$c_{s,\mathrm{min}}^2(\eta,\alpha_0) = \frac{4\alpha_0^2(1-\alpha_0^{-1})^{3/2} - (3-6\alpha_0+4\alpha_0^2)(1-\eta\alpha_0^2)^{3/2}}{4(3-5\alpha_0+2\alpha_0^2)(1-\eta\alpha_0^2)^{3/2} + 8\alpha_0^2(\alpha_0^2\eta-1)(1-\alpha_0^{-1})^{3/2}}\,. \tag{2.21}$$

On Fig. 2 the configuration space of gravastars in equilibrium is illustrated with the help of the dimensionless parameters η and α_0. In explaining the meaning of some of the characteristic curves plotted on Fig. 2 the following considerations seems to be useful.

Returning to the interpretation of some of the curves plotted on Fig. 2 note that the thin dashed, dashed-dotted and thick dashed lines do correspond to configurations for which the square of the speed of sound $c_{\mathrm{s}0}^2$ at α_0 takes the minimal values $c_{s,\mathrm{min}}^2 = 0, w_0, 1$, respectively. Correspondingly, the thick dashed line represents the lower bound of the radius for stable configurations for which the sound speed does not exceed the speed of light. If DEC is also required to hold then α_0 has to be larger than ≈ 1.15028 which is the α_0 value of the configuration represented by point M on Fig. 2.

On Fig. 3 a different representation of the very same configuration space, as depicted on Fig. 2, is given on the $(\Sigma_0, -\Theta_0)$ plane. The points representing stable gravastars by the values (η, α_0) on Fig. 2 are mapped as $(\eta, \alpha_0) \mapsto (\Sigma_0(\eta,\alpha_0), \Theta_0(\eta,\alpha_0))$. The styles

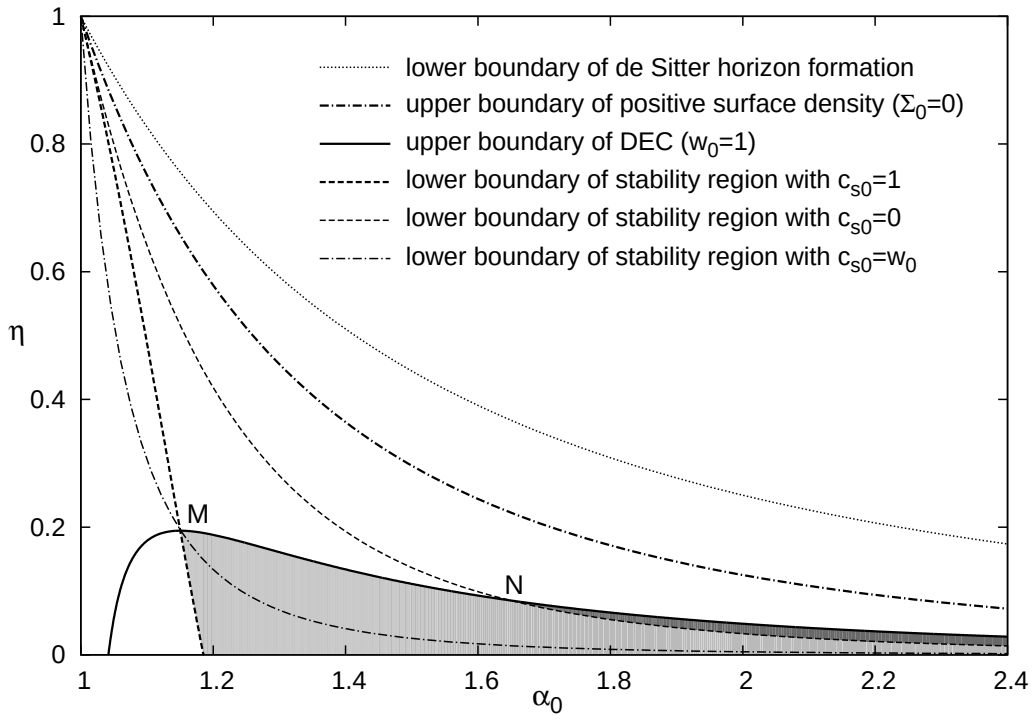

Figure 2. The points below the uppermost dotted line represent configurations where no cosmological horizon may occur in the de Sitter region. At the points of the thick dotted line the surface energy density vanishes. Below that line the proper mass of the shell is always positive. The thick continuous line is determined by equation (2.18) and it shows the upper boundary of the region where DEC holds. This curve meets the horizontal axis at $\alpha_0 = 25/24$ and it has its global maximum at the point M with coordinates $(\alpha_0, \eta) \approx (1.1503, 0.1944)$. The dashed thick line represents configurations with $V''(\alpha_0) \equiv 0$ and with $c_{\rm s0}^2 = 1$. Stability holds, i.e., $V'' > 0$ with $c_{\rm s}^2 = 1$, to the right of this curve, while instable configurations are to the left of this curve. The thin dashed line represents configurations with $V''(\alpha_0) \equiv 0$ and $c_{\rm s0}^2 = 0$. This curve separates also stable and unstable configurations when $c_{\rm s0}$ is restricted to zero. The dashed thin line enters to the DEC region at point N with coordinates $(\alpha_0, \eta) \approx (1.6470, 0.0855)$. On the thin dashed-dot line $V'' \equiv 0$ and $c_{\rm s0}^2 = -\Theta_0/\Sigma_0$ holds. The dashed thick line, the thin dashed-dot line and the curve determining the boundary of the DEC region all intersect at M. Two subregions are indicated by gray shading. In the shaded region stable gravastars can be found within the domain where DEC holds and the speed of sound at α_0 does not exceed the speed of light. The dark gray region represents stable gravastar configurations irrespective of the value of $c_{\rm s0}^2$ until it is non-negative.

of the sheading of the distinguished subregions and that of the characteristic curves and points are in correspondence on these two figures. It is an interesting feature of Fig. 3 that, in virtue of the above argument in connection with $c_{s,\min}^2$, the slope of the tangent at a point of an $\eta = const$ curve is exactly the value of $c_{s,\min}^2$ relevant for the configuration represented by the pertinent point.

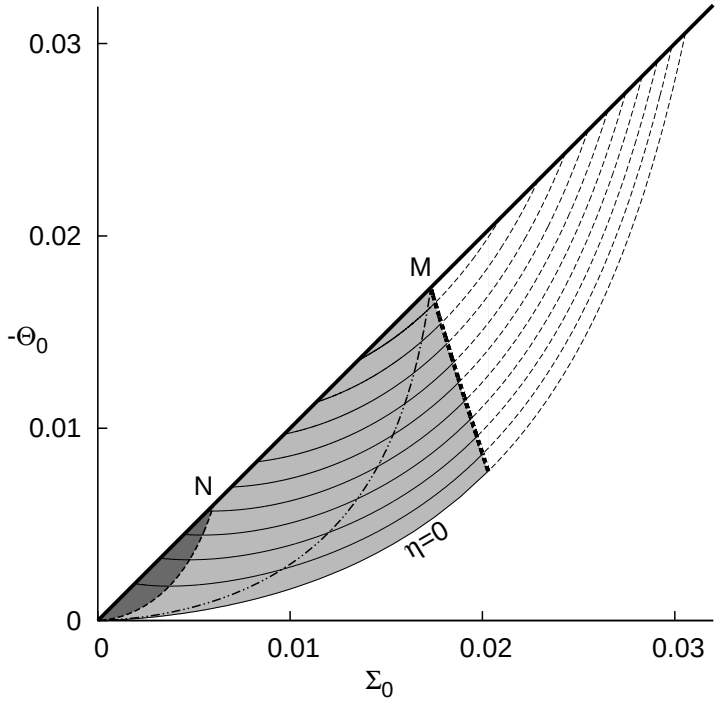

Figure 3. The configuration space of stable gravastars is depicted. An EOS may be represented by a curve on this $(\Sigma_0, -\Theta_0)$ plane. In order to provide a better orientation the $\eta = const$ curves for values ranging from $\eta = 0$ to $\eta = 0.18$, with separation $\Delta\eta = 0.02$, are indicated. The styles of the sheading of the distinguished subregions and that of the characteristic curves and points are the same as they were on Fig. 2.

3. Dust shell falling onto the gravastar

The interaction of a gravastar with a spherical dust shell falling onto it will be studied in this section. In advance to the arrival of the dust shell onto the surface of the gravastar the history of the shell is completely determined by its relativistic equation of motion on a Schwarzschild background. To make our investigations somewhat realistic we shall assume that the collision of the dust shell and the gravastar is totally inelastic, i.e., all the dust particles will be assumed to move together with the surface layer of the yielded dynamical gravastar. In determining its basic parameters—the velocity, mass density, etc.—the conservation of the 4-momenta will be applied. Finally, by inspecting the new potential relevant for the composed system the dynamics of the yielded gravastar can be determined.

According to the above outlined program we shall start with a gravastar in equilibrium the total mass of which M_2 will be used as our reference unit. The dimensionless radius and the mass ratio parameter of this gravastar are $\alpha_0 = a_0/(2M_2)$ and $\eta = 8kM_2^2$, respectively. We assume that a dust shell, with gravitational mass

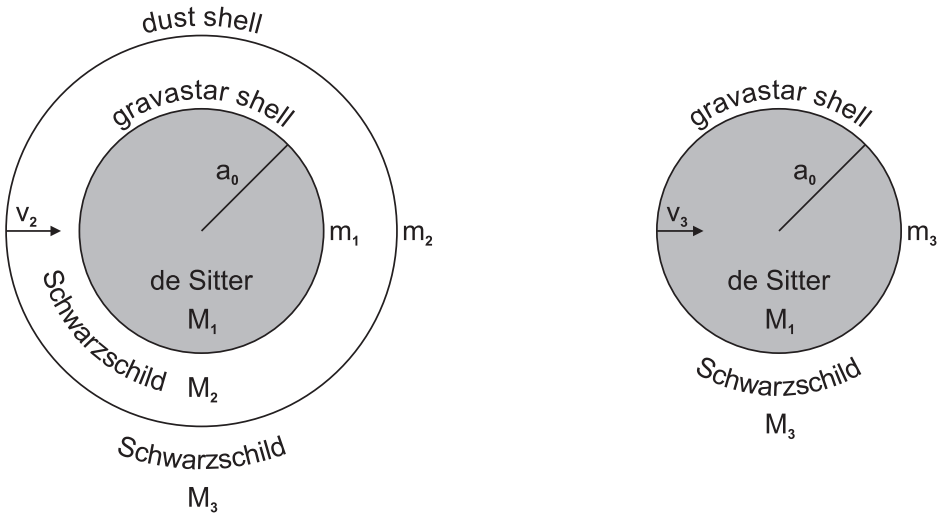

Figure 4. To the left the de Sitter interior with total mass M_1 inside the radius a_0, Schwarzschild exterior with mass parameter M_2 gravastar shell with rest mass m_1 and the moving dust shell with rest mass m_2 are shown. To the right the gravastar the moment of the inelastic collision is indicated.

εM_2, falls onto the surface of the gravastar and the collision between the dust shell and the surface of the gravastar is totally inelastic. This, in particular, means that once the collision occurs a new three-layer dynamical gravastar forms. Fig. 4 is to provide a simple depiction of the underlying process. (For another schematic spacetime diagram see Fig. 6.) Denote the proper mass of the initial shell of the gravastar, of the dust shell and of the shell of the gravastar after the collision by m_1, m_2 and m_3, respectively. To guarantee a_0 to be greater than the Schwarzschild radius of the event horizon of the yielded gravastar—the total mass of which is $M_3 = (1 + \varepsilon)M_2$—, we require the inequality $\varepsilon < \alpha_0 - 1$ to hold.

The dynamical characterization of the dust shell in advance to the collision can be given based on the results outlined in the appendix. Concerning the velocity of the particles of the dust shell at the moment of the collision it will be assumed that either it is equal to the velocity that would be acquired by the shell if it was starting to move towards the gravastar from rest at infinity, i.e., $v_2(\infty) = 0$, or, in the second case, the particles of the dust shell will be assumed to be simply attached to the surface of the gravastar with zero velocity, i.e., $v_2(\alpha_0) = 0$.*

Note that in the $v_2(\infty) = 0$ case the gravitational mass of the dust shell equals to its rest mass, i.e., $m_2 = \varepsilon M_2$ (see the appendix for more details), and also that, in virtue of (A.5), the velocity $v_2 = \mathrm{d}r/\mathrm{d}\tau_2$ at the moment of the collision can be given as

$$v_2 = -\frac{\sqrt{16\alpha_0 + 8\varepsilon\alpha_0 + \varepsilon^2}}{4\alpha_0}\,. \tag{3.22}$$

* Although both of these assumptions correspond to certain limiting cases we expect that they provide some clue about more generic cases with an initial velocity between the two of them.

3.1. Collision

The conservation of the 4-energy-momentum can be used to determine the radial energy and the radial momenta of the surface of the gravastar yielded by the collision. The relevant equations are derived in the Appendix where a detailed and generic investigation of an inelastic collision of two concentric spherically symmetric matter shells is also carried out. Because of spherical symmetry the radial component of the 4-momentum conservation does correspond to the relativistic 3-momentum conservation—given by equation (A.17). In virtue of this relation the radial velocity, $v_3 = \mathrm{d}a/\mathrm{d}\tau_3$, of the boundary of the yielded gravastar if $v_2(\alpha_0) \neq 0$ can be given as

$$v_3 = \frac{8\pi\alpha_0 F(\eta, \alpha_0, \varepsilon)}{\Sigma_3}\,, \tag{3.23}$$

where

$$F(\eta, \alpha_0, \varepsilon) = -\frac{\Sigma_0(\eta, \alpha_0)^2\,(1 - 1/\alpha_0)\,(\varepsilon/2)\,\sqrt{16\alpha_0 + 8\varepsilon\alpha_0 + \varepsilon^2}}{1 - 2\,\eta\,\alpha_0^3 + \eta^2\alpha_0^6 - 4096\,\pi^4\alpha_0^6\,\Sigma_0(\eta, \alpha_0)^4}\,. \tag{3.24}$$

Here $\Sigma_0(\eta, \alpha_0)$ denotes the energy density of the original gravastar in equilibrium given by (2.16).

The temporal component of the 4-momentum conservation corresponds to the energy conservation which can be seen to be equivalent to the dynamical master equation of gravastars (2.2). Using the parameters of the newly formed gravastar the master equation can be given in terms of the above introduced dimensionless parameters as

$$\Sigma_3 = \frac{\sqrt{1 - \eta\alpha_0^2 + v_3^2} - \sqrt{1 - (1 + \varepsilon)/\alpha_0 + v_3^2}}{8\pi\alpha_0}\,. \tag{3.25}$$

The substitution of (3.23) into (3.25) yields then the following equation

$$\Sigma_3 = \sqrt{A(\eta, \alpha_0)^2 + \frac{F(\eta, \alpha_0, \varepsilon)^2}{\Sigma_3^2}} - \sqrt{B(\alpha_0, \varepsilon)^2 + \frac{F(\eta, \alpha_0, \varepsilon)^2}{\Sigma_3^2}}\,, \tag{3.26}$$

with

$$A(\eta, \alpha_0) = \frac{\sqrt{1 - \eta\alpha_0^2}}{8\pi\alpha_0}\,, \quad \text{and} \quad B(\alpha_0, \varepsilon) = \frac{\sqrt{1 - (1 + \varepsilon)/\alpha_0}}{8\pi\alpha_0}\,. \tag{3.27}$$

Equation (3.26) is an algebraic relation for Σ_3 possessing the only positive root

$$\Sigma_3(\eta, \alpha_0, \varepsilon) = \sqrt{A^2 + B^2 - 2\sqrt{A^2B^2 + F^2}}\,, \tag{3.28}$$

where Σ_3 denotes the energy density of the boundary of the newly formed gravastar. Note that the value of Σ_3 is independent from the EOS.

Whenever $v_2(\alpha_0) = 0$ the value of Σ_3 can be determined by (3.25) where the substitution $v_3 = 0$ has to be used.

3.2. After the collision

As discussed above once the collision happened Σ_3 and v_3 can be determined. Note that to be able to determine what happens after the collision we also need to know the EOS of the newly formed surface. Without this information we cannot determine the new surface energy density as a function of the radius, which is essential in assigning the new effective potential.

Concerning the new EOS, since the pressure of the falling dust shell is zero, it is tempting to assume that the surface tension remains intact during the process of collision. This idea could be supported by a simple-minded summation of partial pressures. However, if this happened the particles of the dust should have stopped at the surface of the gravastar without interacting with the particles forming the surface of the gravastar. This appears to be baseless, and more importantly, to be incompatible with the physical picture of inelastic collisions. To resolve the associated discrepancy, hereafter we shall assume that instead of the surface tension the EOS of the boundary remains intact during the inelastic collision. This means that the dust shell "melts" into the matter of the surface of the gravastar.

In determining the new potential, as previously, (2.5) may be applied since after the collision a modified three-layer gravastar is formed. The only distinction is that the new dynamical variables—indicated by tilde—have to be used in (2.5). For the new gravastar $\widetilde{\eta} = (1+\varepsilon)^2\eta$ holds as the mass of the outer Schwarzschild region, used as a reference unit, changes from M_2 to $M_3 = (1+\varepsilon)M_2$. Accordingly, the dimensionless surface density and the dimensionless radius change as $\widetilde{\alpha} = \alpha/(1+\varepsilon)$ and $\widetilde{\Sigma} = (1+\varepsilon)\,\Sigma$. Combining all these observations the new potential may be given as

$$\widetilde{V}(\alpha;\eta) = V((1+\varepsilon)^2\eta, (1+\varepsilon)\Sigma_{\rm new}(\alpha), \alpha/(1+\varepsilon)). \tag{3.29}$$

where $\Sigma_{\rm new}(\alpha)$ is the solution of (2.8) with the initial condition $\Sigma_{\rm new}(\alpha_0) = \Sigma_3$ provided that the EOS remains intact as we assumed to be the case.

4. Results

By inspection of the new effective potential the dynamics of the gravastar can be determined. If the new potential possesses the form of graphs 2 of Fig. 1 the motion of the gravastar surface remains bounded and we can determine the minimum and maximum value of the radius. In particular, the maximum mass which may be dropped onto the original gravastar without converting it into a BH can also be determined. In this case the potential for a maximally loaded gravastar takes the form of graph 3 of Fig. 1.

4.1. The applied method

Note first that if $v_2(\alpha_0) \neq 0$ after collision the initial velocity points inward (unless $v_2(\alpha_0) = 0$), therefore the investigation has to start by deriving whether the new effective

potential has any root in the interval $\alpha \in [1, \alpha_0]$. If not then an event horizon will form and the gravastar collapses to a BH. The examination of the potential is made by a numerical maximum finding algorithm. If the maximum is found to be less than zero, the collapse to a BH will occur. Using an interval bisection method, changing the initial gravitational mass of the dust shell to be dropped, the numerical value of the maximal gravitational mass, $\varepsilon_{\max} \cdot M_2$, which may fall onto the gravastar without converting it into a BH can be determined. Whenever $v_2(\alpha_0) \neq 0$ and there is a root in the interval $\alpha \in [1, \alpha_0]$, the motion gets to be bounded and it happens so that $\alpha_1 \leq \alpha \leq \alpha_2$, where α_1 is the largest root that is smaller than α_0 and α_2 is the smallest root that is larger than α_0. If $v_2(\alpha_0) = 0$ then α_0 coincides with either the upper or lower bound of the motion.

It is an inherent property of the gravastar model that we cannot have information about the de Sitter energy density inside the gravastar, η, neither about the EOS of the shell before and after the collision. To have some quantitative results suitable hypotheses have to be applied. In order to avoid the use of a flood of parameters—each of which has to possess definite values in numerical investigations—, as indicated in Section 2.3, in this paper we analyze three types of EOS: homogeneous linear, broken linear and polytrop.

If we fix an EOS with all of its parameters, then, as a function of η, the stable equilibrium radius, α_0, gets to be determined. Note, that this radius can be determined by the intersection of the specific EOS curve and the corresponding η-level curve on the Fig. 3. Next we have to make an assumption about the EOS after the collision. Since we have no observational clues, as it was indicated above, we shall assume that the EOS remains intact, which means that the dust shell melts into the matter of the gravastar shell yielding an increase of the pressure according to its mass contribution. Note that in case of an initially homogeneous linear EOS the possibility of keeping the surface tension to be intact will also be investigated. Note that this latter case might be a good approximation whenever the contribution of the dust shell to the new shell's composition is negligible.

4.2. Homogeneous linear EOS

As it was mentioned in Subsection 2.3, the simplest possible EOS is the homogeneous linear one. If the value of η and w_0 are given that of α_0 gets to be determined by the implicit relation $w_0 = -\Theta_0(\eta, \alpha_0)/\Sigma_0(\eta, \alpha_0)$. It is clearly visible on Fig. 3 that for a given value of w_0 $(= c_s^2 \in [0, 1])$ the $w_0\,\Sigma_0 + \Theta_0 = 0$ line intersects any η constant curve at most at two points. One of these intersections corresponds to a stable configuration, with the smaller Σ_0 value, while the other is unstable. Accordingly, once the choice for η and w_0 is done first we determine the value of α_0 by solving numerically the implicit relation $w_0 = -\Theta_0(\eta, \alpha_0)/\Sigma_0(\eta, \alpha_0)$. Then, for any choice of the pair (η, w_0), we determine the stable gravastar configuration, and as it was outlined above, the maximal mass of the shell that can be dropped onto it without converting it into a BH can also

be determined. The results of the corresponding investigations are depicted by Fig. 5. It is worth to be mentioned that some of the special cases depicted on these panels play distinguished role in various arguments. For instance, the case $w_0 = 1/3$ corresponds to ultrarelativistic gas, which—based on certain dimension reduction arguments that might not be straightforward to be applied in the present case—is represented in [24] by a system with $w_0 = 1/2$.

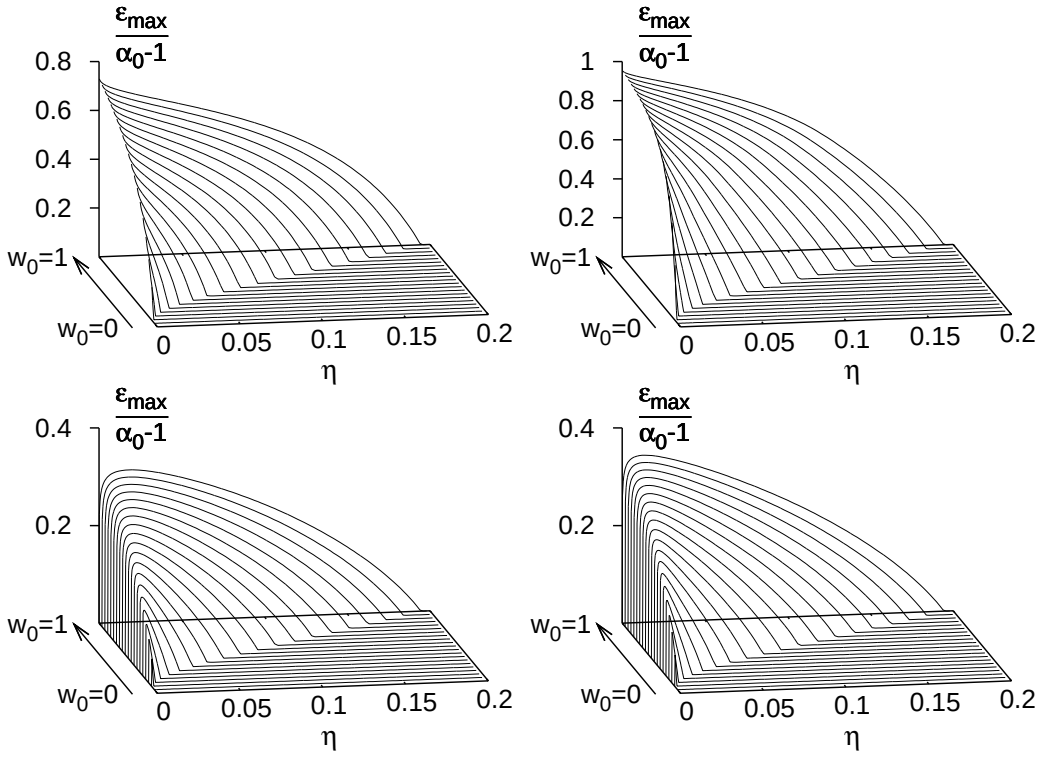

Figure 5. The normalized value $\varepsilon_{\max}/(\alpha_0 - 1)$ is shown as a function of η and w_0 for homogeneous linear EOS, where α_0 stands for the maximal dimensionless radius allowed by DEC. On the top two panels $v_2(\infty) = 0$, while on the bottom two ones $v_2(\alpha_0) = 0$. The panels to the left depict the intact EOS cases, while on the right ones the surface tension was kept to be intact.

Note that to have a stable configuration the value of $w_0 = c_s^2$ has to be larger than $c_{s,\min}^2$ given by (2.21). In particular, $w_0 = c_s^2$ may take all the values from the interval $[0, 1]$ only for $\eta = 0$, i.e., whenever the inner region is vacuum. Note also that $\varepsilon_{\max}$ has to be smaller than $\alpha_0 - 1$. If $\varepsilon \geq \alpha_0 - 1$ occurred the system composed by the gravastar and the dust shell would get beyond its own Schwarzschild radius before the collision happened. This makes the use of the rescalled quantity $\varepsilon_{\max}/(\alpha_0 - 1)$ to be advantageous.

Before interpreting Figs. 5 and 6 let us recall that a homogeneous linear EOS, $\Theta_0 = -w_0\,\Sigma_0$, has w_0 as the only parameter. Therefore, it is also straightforward to investigate the case when both the surface tension and the functional form of the EOS remain intact during the collision. It is done by determining the value of the new $\widetilde{w}_0$ via the relation $\widetilde{w}_0 = -\Theta_0/\Sigma_3$. If this happens the particles of the dust shell do not

adopt the properties of the particles comprising the surface of the gravastar as only the rest mass of the surface will be increased by the collision. On both Figs. 5 and 6 four different subcases are considered. These subcases are yielded, on the one hand, by keeping the EOS or the surface tension to be intact and, on the other hand, by choosing the velocity of the particles of the dust shell at the moment of the collision to be such that either $v_2(\infty) = 0$ or $v_2(\alpha_0) = 0$, as discussed in Section 3.

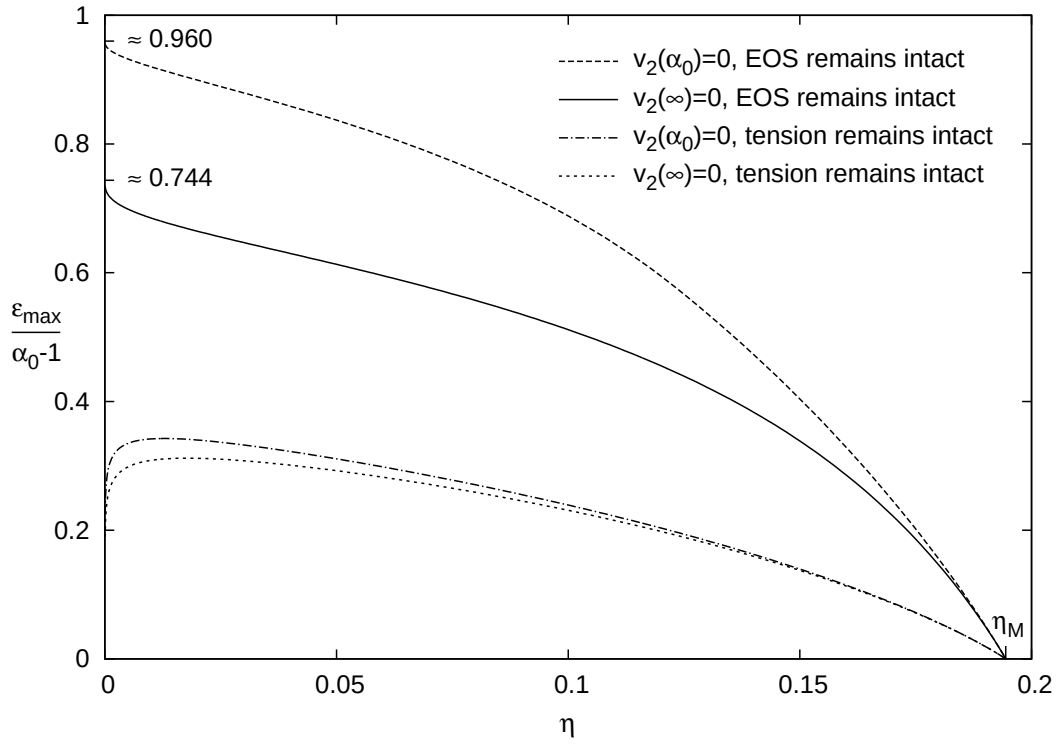

Figure 6. The $w_0 = 1$ sections of the four panels of Fig. 5 are shown providing a better comparison of $\varepsilon_{\max}$ for the considered configuration. The order of the curves from top to bottom coincides with that of the legend at the upper right corner.

Figs. 6 depict only the $w_0 = 1$—referred as stiff matter in [8]—sections of the four cases indicated on Fig. 5 which offers a better comparison of the corresponding four different dynamical subcases. Fig. 7 does also refer to these four basic configurations with $w_0 = 1$. The horizontal sections, corresponding to an $\eta = const$ value, of the grey regions indicate the dynamical range of the radius of gravastars. For the particular value $\eta = 0.05$ the pertinent new potentials are also indicated.

There are two interesting points to be mentioned that are indicated by Fig. 7. First, there are two dotted vertical lines on each of the panels. The one with the larger α value corresponds to the Buchdahl limit with $\alpha = 9/8$ [25], while the one with smaller α value indicates the corresponding lower bound, with $\alpha \approx 1.0384$, to the size of most compact conventional stars. On these panels of Fig. 7 it is also visible that dynamical gravastars cannot get below the Buchdahl limit so they definitely remains less compact than the most compact conventional stars satisfying DEC.

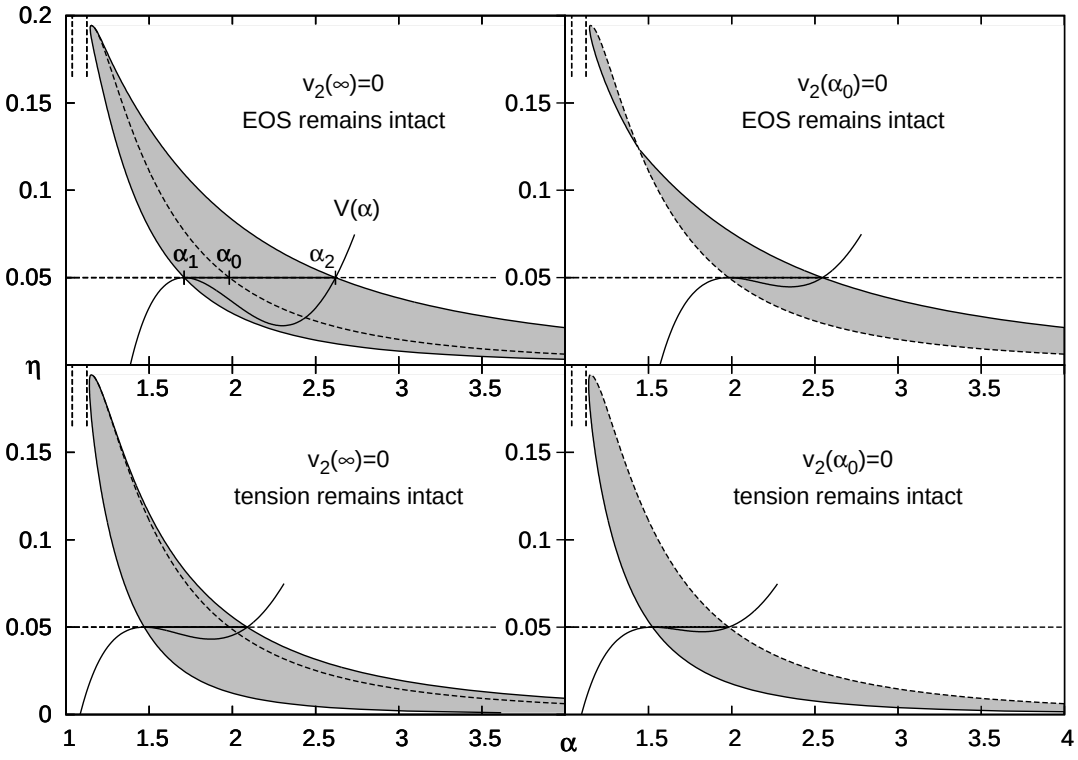

Figure 7. The dynamical range of the radius for maximally loaded gravastars are shown referring to the four basic configurations with $w_0 = 1$ considered on Fig. 6. The $\eta = const$ sections of the gray regions giverepresent the dynamical range of the radius relevant for the considered four subcases. The η dependence of α_0 of the gravastars in advance to the collision is indicated by the dashed curves. Whenever the initial velocity of the dust shell is nonzero (e.g., $v_2(\infty) = 0$) the dashed line is in the interior of the grey region, whereas whenever $v_2(\alpha_0) = 0$—see, e.g., the right panels—the gravastar stars its motion at the edge (minimal or maximal α value) of the dynamical range. For the particular choice $\eta = 0.05$ the corresponding potentials, are also plotted, where the zeros of the potentials are indicated by the dotted horizontal lines and the applied scales are the same on each of these panels. The dotted vertical line with the larger $\alpha = 9/8$ value correspond to the Buchdahl limit, while the other one with $\alpha \approx 1.0384$ indicates the corresponding lower bound to the size of most compact conventional stars satisfying DEC.

Second, on the right two panels with $v_2(\alpha_0) = 0$ the grey regions on one side are bounded by the dashed lines representing the η dependence of α_0 of the initial gravastar. This is, on one hand, in accordance with intuition as the particles of the dust shell are simply simultaneously placed on the surface of the gravastar. What might be unexpected, on the other hand, is the following. Whenever the EOS remains intact (see the right-top panel of Fig. 7) there is a subregion where the dashed line bounds from above and another where it bounds from below ♯—these subregions are separated by a

♯ The response of the initial gravastar for the placement of the dust shell onto its surface is as follows: By increasing the value of ε from zero to $\varepsilon_{\max}$ first the radius increases. However, for configurations with $\alpha_0 < 1.44$ there is a turning point in α and before reaching $\varepsilon_{\max}$ the radius gets to be smaller than the initial α_0.

point $(\eta, \alpha_0) \approx (0.124, 1.44)$ where the initial gravastar remains apparently at rest for $\varepsilon = \varepsilon_{\max}$—, while whenever the surface tension remains intact—as it is indicated by the right bottom panel of Fig. 7—the dynamical range for $\varepsilon = \varepsilon_{\max}$ is always bounded from above by the initial gravastar configurations.

4.3. Broken linear EOS

Since the gravastar radius has always to decrease at the moment of the collision the surface density must increase at this moment. Thus, the functional form of the new effective potential depends only on that of the EOS relevant for mass density greater than Σ_0. Motivated by this observation we have used the following particular broken linear EOS. $\Sigma_0(\eta, \alpha_0)$ was chosen to be the breaking point, i.e., the choice $\Sigma_1 = \Sigma_0$ was made, and only the slope was varied for $\Sigma > \Sigma_0$. Since we have found that the higher the value of w_0 the more stable is a gravastar the broken linear EOS we have chosen $w_1 = 1$ and varied w_2 form zero to 1, in steps 0.1, as it is indicated on the right panel of Fig. 8.

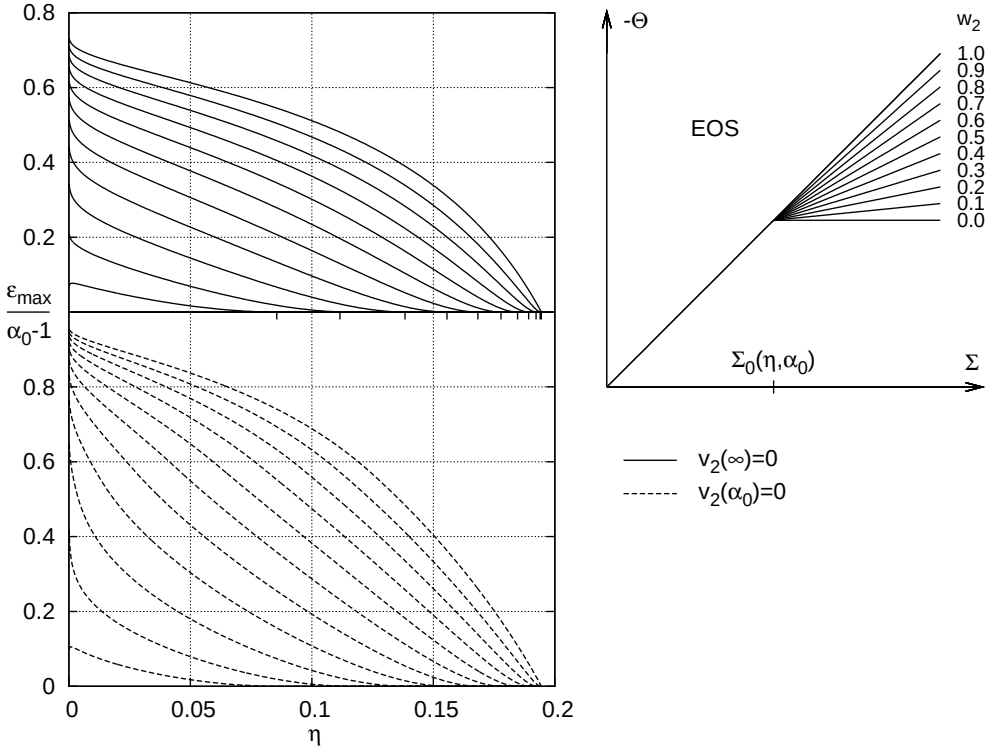

Figure 8. The applied broken linear EOS is shown on the top right panel. α_0 is chosen to be maximal such that DEC is still guaranteed to hold. On the graphs of the left panels the value of w_2 decreases form one to zero, in steps 0.1, while moving downwards.

On Fig. 8 the η dependence of $\varepsilon_{\max}$, i.e, the maximal value of the gravitational mass of the shell that may be dropped onto a stable gravastar without converting it into a BH is shown for configurations with $v_2(\infty) = 0$ and $v_2(\alpha_0) = 0$. On both of the left

panels the value of w_2 decreases from one to zero while moving from the top to the bottom. It is also visible that for each particular value of w_2 there is a maximal value of η that is indicated by the vertical ticks on the horizontal axis of the the top left panel. These figures do also justify—for the pertinent linear approximation of the EOS—that for given η and α_0 the larger the value of $c_{s0} = w_2$ is the more stable the gravastar gets in the sense that the allowed value of $\varepsilon_{\max}$ increases together with c_{s0}.

4.4. Polytrop EOS

A polytrop EOS of the form of (2.14) has two parameters, A and κ. Given a point (Σ_0, Θ_0)—with $0 < |\Theta_0| < \Sigma_0$—it is not obvious to choose at all the parameters A and κ to get an EOS fitting to this point except for the choice $\kappa = 2$. To overcome this slight technical difficulty and also to apply the simplest possible choicebecause for a given value of A always the choice $\kappa = 2$ yields the most stable configuration we have chosen $\kappa = 2$ and varied only the value of A. It is also informative to compare the behavior of a gravastar with a polytrop EOS and with a linear one having the same slope at Σ_0 as it is indicated by the nested panel on Fig. 9 relevant for the particular choice $\kappa = 2$. For any choice of η the value of α_0 is chosen to be determined by the intersection of the $\eta = const$ line and the dashed-dotted curve on Fig. 2. Note that if α_0 was chosen to be the maximal value for a given η such that DEC holds the polytrop EOS would degenerate to the homogeneous linear one with $w_0 = 1$.

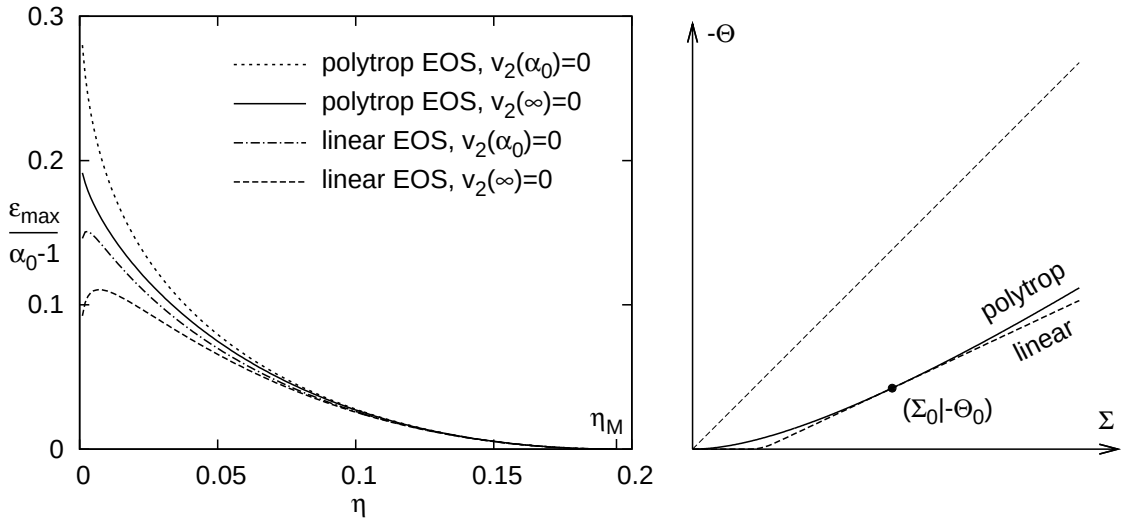

Figure 9. On the right the applied polytrop EOS with $\kappa = 2$ and the linear one, having the same slope at Σ_0 are illustrated. For any choice of η the corresponding value of α_0 is determined by the intersection of the $\eta = const$ line and the dashed-dotted curve on Fig. 2. The η dependence of $\varepsilon_{\max}/(\alpha_0 - 1)$ is shown for two types of EOS and for the two types of initial velocities, $v_2(\infty) = 0$ and $v_2(\alpha_0) = 0$. On the left panel the order of the curves from top to bottom coincides with that of the legend at the upper right corner.

The η dependence of the maximum of the normalized gravitational mass of the

dust shell, $\varepsilon_{\max}/(\alpha_0-1)$,—where $\varepsilon_{\max}$ is the maximal mass that may be dropped onto a gravastar without converting it into a BH—is shown on Fig. 9 for two types of EOS and for the two types of choices concerning the initial velocities, $v_2(\infty)=0$ and $v_2(\alpha_0)=0$. As it might have been anticipated, Fig. 9 justifies that a gravastar characterized by a polytrop EOS is more stable than the corresponding one with linear EOS in consequence of the fact that the slope of the polytrop EOS is larger than that of the linear one for $\Sigma>\Sigma_0$.

5. Conclusions

In this paper, besides providing a short survey of gravastars in equilibrium, the radial stability of gravastars was investigated. The latter was done by determining the response of a gravastar to the arrival of a dust shell onto its surface. Concerning the matter model of the surface of the gravastar three different types of EOS were applied. We also assumed that DEC holds and the speed of sound c_s satisfies the relations $0\leq c_s\leq 1$.

Our most important findings are as follows: Among the investigated EOSs the homogeneous linear one with $c_s=1$ appears to provide the mostlargest possible stable states stability for a gravastars in the sense that for a chosen η the value of $\varepsilon_{\max}$ attains its largest possible value for $c_s=1$. It would be interesting to find an analytic justification of this observation. It also follows from our investigations that once an EOS is fixed, for a given value of α_0, the smaller the value of η is, or alternatively, for a given value of η, the larger the value of α_0 is the more stable is a gravastar. The maximal mass of the shell that may be dropped onto a gravastar in equilibrium without converting it into a BH is also determined. The normalized value of this gravitational mass $\varepsilon_{\max}/(\alpha_0-1)$ was found to be the largest $\varepsilon_{\max}/(\alpha_0-1)\approx 0.96$ whenever the matter comprising the surface of the gravastar possesses a homogeneous linear EOS with $w_0=1$ and $v_2(\alpha_0)=0$. It should be noted that, in general, the value of $\varepsilon_{\max}$ may be huge for sufficiently small value of η but this also come along with enormously large radius of the gravastar. This latter type of gravastars are, however, far away from the state of being considered as alternatives to BHs. Correspondingly the value of $\varepsilon_{\max}\approx 0.96\cdot(a-2M)/2M$ is of the order M for a gravastar with radius $a\approx 3M$ which indicates that gravastars may be significantly more stable (although not smaller) than ordinary stars. It is also important to note that, in general, the value of $\varepsilon_{\max}$ may be huge for sufficiently small value of η but this also come along with enormously large radius of the gravastar

In the appendix a generic framework describing the totally inelastic collision of two shells is also worked out. The reason behind considering inelasticity collisions is that the de Sitter region of a gravastar is unstable against hydrodynamical excitations. Thereby, it was reasonable to assume that the particles of the dust shell merge to the particles of the surface of the gravastar. In most of the considered cases, for the sake of simplicity, we also assume that the EOS of the surface of the gravastar remains intact during the collision. All these assumptions indicate that there might be various generalizations of the simple model we applied. Nevertheless, our findings in all the

investigated cases clearly manifest that even a dynamical gravastar cannot be more compact than the smallest possible ordinary stars of the same mass provided that for both types of models DEC is guaranteed to hold. †† This means that the main issue is not that whether gravastars can be distinguished from a BH. Assuming that they exist in reality it is more appropriate to ask whether they can be distinguished from compact regular stars.

Let us finally turn the case of a generic BH mimicing gravastar without restricting our considerations by referring to DEC or to any particular EOS of the surface layer. Note that in this case the size of the gravastar is not bounded from below so, in particular, the assumption $\alpha_0 \approx 1$ corresponding to the requirement of Mazur and Mottola may also hold. Assume now that the mass of this gravastar is M and that the gravitational mass of the dust shell—falling onto it—is $\varepsilon \cdot M$. For simplicity we assume that the particles of the dust shell moves towards the gravastar with velocity as if they started from rest at infinity, i.e., $v_2(\infty) = 0$. Then, the mass of the composed system is $(1+\varepsilon)M$. In order to avoid the situation in which the composed system gets beyond its own Schwarzschild radius $R_S = 2(1+\varepsilon)M$, in advance to the collision, for the radius of the initial gravastar, $R_{\alpha_0} = 2\alpha_0 M$, the inequality $R_S < R_{\alpha_0}$ must hold. This immediately implies then that $\varepsilon < \alpha_0 - 1$, and in turn that the closer of the radius of the initial gravastar is to the Schwarzschild radius the smaller the mass of the dust shell, which may be dropped onto it without converting it into a BH, must be. In other words, the better is a gravastar in mimicing a BH the easier is to destroy it by the described process. Note that since this argument does not refer to the internal structure of the gravastar model it applies not only to the simplified three-layer model of Visser and Wiltshire or to the original model of Mazur and Mottola but essentially to any analogous construction.

Acknowledgments

This research was supported in part by OTKA grant K67942.

Appendix

This appendix is to introduce the basic equations governing the dynamics of a totally inelastic collision of a pair of concentric spherical shells the outer of which is moving in a vacuum spacetime region. These equations are derived by making use of the conservation of 4-momentum. In determining them we have applied a suitable adaptation of the method of Nakao, Ida and Sugiura which was originally worked out in [27] to describe the conservation of 4-momentum in the special case of totally transparent shell crossings. In what follows the abstract index notation will be applied. In particular, the lowercase

††It is known for long that a gravastar—neither in the shell based model nor in its continuum correspondence—can be of considerably smaller size unless DEC is violated [10, 26].

Latin indices will indicate the type of tensors while Greek indices will refer to the components of tensors with respect to some specified basis fields.

To start off consider two spherically symmetric concentric shells. Each of these shells is assumed to be infinitely thin and their history (before the collision) are assumed to be represented by separate timelike hypersurfaces. These hypersurfaces will also be referred as shells hereafter. Once the collision happens it is assumed that the initial shells merge such that a single infinitesimally thin shell is formed. As it is depicted by the simple schematic picture on Fig. 6 the spacetime may be divided into three characteristically different regions. In advance to the collision shell 1 and shell 2 indicate

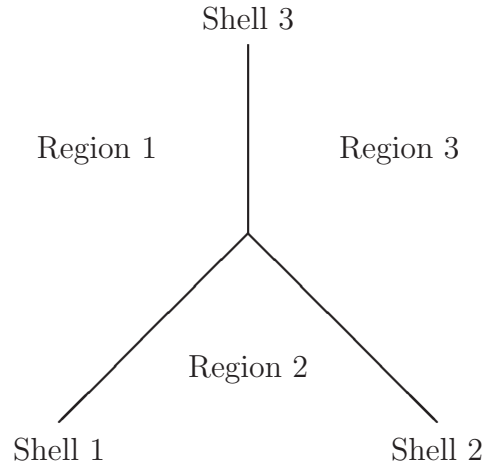

Figure 6. A schematic spacetime diagram representing a totally inelastic collision. The vertical direction is temporal and time progress upward.

the interior and exterior shells, respectively, while the shell yielded by the merging of these two shells is represented by shell 3. The inside spacetime region which has shells 1 and 3 on its the boundary is called region 1, the region between shells 1 and 2 is called region 2, while the outside region bounded by shells 2 and 3 is called region 3. For notational convenience we introduce region 4 which is identical to region 1. Hereafter we use capital Latin index K to indicate the label either of a shell or of a region. Accordingly, the value of K runs from 1 to 3 unless otherwise stated.

The metric in the disjoint spherical symmetric regions, labelled by K, will be assumed to be given as

$$\mathrm{d}s_K^2 = -f_K(r)\mathrm{d}t^2 + f_K(r)^{-1}\mathrm{d}r^2 + r^2\mathrm{d}\Omega^2, \tag{A.1}$$

with

$$f_K(r) = 1 - \frac{2M_K(r)}{r}. \tag{A.2}$$

Note that this class is generic enough to include both the Schwarzschild and de Sitter vacuum spacetimes, but the electrovacuum Reisner-Nordström solution does also fit to this form.

In restricting our attention to a system consisting of a gravastar and a spherical shell falling onto it—this is the very system investigated in this paper—in regions 2 and 3, in virtue of Birkhoff's theorem, the metric has to be (locally) isometric to that of the Schwarzschild spacetime. Accordingly, in regions 2 and 3 the metric can be given by (A.1) and (A.2) with $M_K(r) = M_K$, where the constants M_K denote the corresponding gravitational mass parameters of the pertinent Schwarzschild spacetimes. In addition, in region 1 the metric is (locally) isometric to the de Sitter spacetime with $M_1(r) = (4\pi/3)\rho_0\, r^3$, where ρ_0 is the energy density in the de Sitter vacuum. In this case case M_3 stands for the total gravitational mass of the system, while M_2 denotes the total gravitational mass of the entire system.

Note, however, that in carrying out the following calculations there is no need to make any specific choice, i.e., the metric in region 1 will only be required to possess the form (A.1) and (A.2). This provides us the freedom that whenever the interior is chosen to be de Sitter type the corresponding equations will immediately be applicable to a system formed by a shell falling onto a gravastar, while if the interior is chosen to be Schwarzschild type the relevant equations describe the inelastic collision of two confocal spherical shells in a Schwarzschild vacuum spacetime.

In proceeding denote by u^a_K the 4-velocity of shell K. The components of the 4-velocity, with respect to the coordinates in regions bounding shell K, can be given as

$$u^\alpha_{K(\pm)} = \left(\frac{\mathrm{d}t_{K(\pm)}}{\mathrm{d}\tau_K}, \frac{\mathrm{d}r_K}{\mathrm{d}\tau_K}, 0, 0\right), \tag{A.3}$$

where τ_K denotes the proper time on shell K and the suffixes $(+)$ or $(-)$ indicate whether the pertinent region is outside or inside with respect to shell K. Note that—as opposed to the area radius, r, which is everywhere continuous—the time coordinate is not continuous across a shell. Once the components of u^a_K are fixed the spacelike outward pointing unit vector, n^a_K, normal to shell K can be determined by the orthogonality condition, $n_{Ka}u^a_K = 0$, and its components can be given as

$$n^\alpha_{K(\pm)} = \left(\frac{\mathrm{d}r_K/\mathrm{d}\tau_K}{f_{(\pm)}(r)}, f_{(\pm)}(r)\frac{\mathrm{d}t_{K(\pm)}}{\mathrm{d}\tau_K}, 0, 0\right). \tag{A.4}$$

The evaluation of (A.3) and (A.4) requires the determination of the radial velocity, $\mathrm{d}r_K/\mathrm{d}\tau_K$. There are various ways to get the value of $\mathrm{d}r_K/\mathrm{d}\tau_K$. The most widely known method is based on the thin-shell formalism of Israel-Sen-Lanczos-Darmois. For a comprehensive summary of this formalism see [8]. After an appropriate reformulation of the "master equation" (see equation (38) of [8]), which is in fact an energy balance equation, $\mathrm{d}r_K/\mathrm{d}\tau_K$, can be given as

$$\left(\frac{\mathrm{d}r_K}{\mathrm{d}\tau_K}\right)^2 = \frac{g_K(r)^2}{m_K(r)^2} - 1 + \frac{M_K(r) + M_{K+1}(r)}{r} + \frac{m_K(r)^2}{4r^2}\,, \tag{A.5}$$

where $m_K(r)$ denotes the rest mass, while $g_K(r)$ stands for the gravitational mass of shell K. Accordingly, $g_K(r) = M_{K+1}(r) - M_K(r)$ for $K = 1, 2$ and $g_3(r) = M_3(r) - M_1(r)$.

Note that the rest mass of the shell of a gravastar, in general, is a function of the area radius, nevertheless, the rest mass of a dust shell is constant.

Recall that the components of the 4-velocity cannot be independent as $u_{Ka}u_K^a = -1$ which, in particular, implies that

$$\frac{\mathrm{d}t_{K(\pm)}}{\mathrm{d}\tau_K} = \frac{\sqrt{(\mathrm{d}r_K/\mathrm{d}\tau_K)^2 + f_{(\pm)}(r)}}{f_{(\pm)}(r)}\,. \tag{A.6}$$

The substitution of (A.5) into (A.6), and some straightforward algebraic manipulations, yields that

$$\frac{\mathrm{d}t_{K(\pm)}}{\mathrm{d}\tau_K} = \frac{g_K(r) \mp h_K(r)}{m_K(r) f_{K(\pm)}(r)}\,, \tag{A.7}$$

where $h_K(r) = m_K^2(r)/2r$, referred as the self-gravity of shell K.

Returning to the main line of the argument recall that our aim is to determine the motion of the shell yielded by the merging of the two initial ones. In doing so the only guiding principle we can use is the conservation of 4-momentum

$$m_3 u_3^a = m_1 u_1^a + m_2 u_2^a\,, \tag{A.8}$$

which has to be evaluated at the moment of the collision. Note that the content of (A.8) is nothing but two scalar equations. The temporal component corresponds to the energy conservation, while the radial component expresses to the radial momentum conservation. The other two components vanish identically due to the spherical symmetry. The two non-trivial equations completely determine the motion of the outgoing shell since, as we shall see below, both the radial velocity and the rest mass m_3 get to be fixed by them. Note that since the collision is inelastic a part of the kinetic energy is converted into binding energy which, in particular, implies that $m_3 \neq m_1 + m_2$.

In applying (A.8) each of the 4-velocities have to be expressed with respect to a common coordinate basis field. Start by choosing the coordinate basis field of region 1 as our reference frame. Then, in virtue of (A.3), the formal expressions of the components of u_1^a and u_3^a get immediately be determined. Similarly, in virtue of (A.3) and (A.4), the coordinate basis components of u_1^a and n_1^a of region 1 are known, therefore u_2^a may be expressed there as the linear combination

$$u_2^a = -(u_2^b u_{1b})\, u_1^a + (u_2^b n_{1b})\, n_1^a\,. \tag{A.9}$$

By applying (A.1), (A.2), (A.3) and (A.4)

$$n_{K(\pm)\alpha} = \left(-\frac{\mathrm{d}r_K}{\mathrm{d}\tau_K}, \frac{\mathrm{d}t_{K(\pm)}}{\mathrm{d}\tau_K}, 0, 0\right). \tag{A.10}$$

$$u_{K(\pm)\alpha} = \left(-f_{(\pm)}(r)\frac{\mathrm{d}t_{K(\pm)}}{\mathrm{d}\tau_K}, \frac{\mathrm{d}r_K/\mathrm{d}\tau_K}{f_{(\pm)}(r)}, 0, 0\right), \tag{A.11}$$

which, along with the notation $p_K = m_K(\mathrm{d}r_K/\mathrm{d}\tau_K)$, implies that

$$u_2^b u_{1b} = \frac{p_1 p_2 - (g_1 - h_1)(g_2 + h_2)}{m_1 m_2 f_2}\,, \tag{A.12}$$

$$u_2^b n_{1b} = \frac{(g_1 - h_1)p_2 - (g_2 + h_2)p_1}{m_1 m_2 f_2}\,. \tag{A.13}$$

By substituting these relations into (A.9) the components of u_2^a in region 1 gets to be determined. Finally, by making use of these components, along with (A.7), the two non-trivial equations in (A.8) can be given as

$$h_3 - g_3 = h_1 - g_1 - \frac{(g_2 + h_2)(p_1^2 - g_1^2 + h_1^2) + 2p_1 h_1 p_2}{m_1^2 f_2}\,, \tag{A.14}$$

$$p_3 = p_1 - \frac{p_2(p_1^2 - g_1^2 + h_1^2) + 2p_1 h_1 (g_2 + h_2)}{m_1^2 f_2}\,, \tag{A.15}$$

where g_3 can be eliminated from (A.14) by using the relation $g_3 = g_1 + g_2$. We would like to emphasize that in deriving these relations no use of the EOS of the shells has been made.

Let us finally restrict our considerations to the case of a dust shell falling onto a gravastar. Since the gravastar is in equilibrium $p_1 = 0$. Thus, in virtue of (A.15), we get

$$m_3 v_3 = m_2 v_2 \frac{g_1^2 - h_1^2}{m_1^2 f_2}\,. \tag{A.16}$$

Whenever $v_2 = 0$ then $v_3 = 0$ also holds. Whenever $v_2 \neq 0$ and the gravitational mass of the shell is equal to its proper mass—in this case $v_2(\infty) = 0$—by making use of the notation of Section 3 the relations $m_2 = \varepsilon M_2$, $m_3 = 4\pi(\alpha_0 2M_2)^2\Sigma_3/M_2$, $f_2 = 1 - 1/\alpha_0$, $g_1 = M_2(1 - \eta\alpha_0^3)$ and (3.22) can also seen to be hold. By substituting them into (A.16) the radial velocity, v_3, of the shell, at the moment of the collision, can be written as

$$v_3 = -\frac{4\pi\,\Sigma_0^2\,(\alpha_0 - 1)\,\varepsilon\,\sqrt{\varepsilon^2 + 8\,\varepsilon\,\alpha_0 + 16\,\alpha_0}}{\Sigma_3\,(1 - 2\,\eta\,\alpha_0^3 + \eta^2\alpha_0^6 - 4096\,\pi^4\alpha_0^6\,\Sigma_0^4)}\,. \tag{A.17}$$

References

[1] Celotti A, Miller J C and Sciama D W 1999 *Astrophysical evidence for the existence of black holes*, *Class. Quantum Grav.* **16** A3

[2] Kormendy J 2003 *The Stellar-Dynamical Search for Supermassive Black Holes in Galactic Nuclei*, Carnegie Observatories Astrophysics Series, Vol. 1: *Coevolution of Black Holes and Galaxies*, ed. L. C. Ho (Cambridge: Cambridge Univ. Press)

[3] Melia F 2005 Astronomy: *Odd company*, Nature **437** 1105

[4] Visser M 2009 *Black holes in general relativity*, Preprint: gr-qc/0901.4365

[5] Mazur P O and Mottola E 2001 *Gravitational vacuum condensate stars*, Preprint: gr-qc/0109035

[6] Frolov V P, Markov M A and Mukhanov V F 1988 *Through a black hole into a new universe?*, Physics Letters B **216** 272

[7] Balbinot R and Poisson E 1990 *Stability of the Schwarzschild–de Sitter model*, *Phys. Rev.* D **41** 395

[8] Visser M and Wiltshire D L 2004 *Stable gravastars - an alternative to back holes?*, *Class. Quantum Grav.* **21** 1135
[9] Israel W 1966 *Singular hypersurfaces and thin shells in general relativity*, Nouvo Cimento B **44** 1; 1967 Nouvo Cimento B **48**, 463 (erratum)
[10] Cattoen C, Faber T and Visser M 2005 *Gravastars must have anisotropic pressures*, *Class. Quantum Grav.* **22** 4189
[11] Carter B M N 2005 *Stable gravastars with generalized exteriors*, *Class. Quantum Grav.* **22** 4551
[12] Bilić N, Tupper G B and Viollier R D 2006 *Born-Infeld phantom gravastars*, J. Cosmol. Astropart. Phys. **02** 013
[13] Horvat D, Ilijić S and Marunović A 2009 *Electrically charged gravastar configurations*, *Class. Quantum Grav.* **26** 025003
[14] DeBenedictis a et al 2006 *Gravastar Solutions with Continuous Pressures and Equation of State*, *Class. Quantum Grav.* **23** 2303
[15] Chirenti C B M H and Rezzolla L 2007 *How to tell a gravastar from a black hole*, *Class. Quantum Grav.* **24** 4191
[16] Rocha P, Miguelote A Y, Chan R, Silva M F A, Santos N O and Wang A 2008 *Can gravastars be formed from gravitational collapse?*, Preprint: gr-qc/0803.4200
[17] Rocha P, Miguelote A Y, Chan R, Silva M F A, Santos N O and Wang A 2008 *Bounded excursion stable gravastars and black holes*, J. Cosmol. Astropart. Phys. **6**, 025
[18] Sen N 1924 *Über die Grenzbedingungen des Schwerefelds an unstetig Keistflächen*, Ann. Phys. (Leipzig) **73** 365
[19] Lanczos K 1924 *Flächenhafte verteiliung der materie in der Einsteinschen gravitationstheorie*, Ann. Phys. (Leipzig) **74** 518
[20] Darmois G 1927 *Mémorial des Sciences Mathématiques*, Gauthier-Villars, Paris, France Vol. 25
[21] Barceló C and Visser M 2002 *Twilight for the energy conditions?*, Int. J. Mod. Phys. D **11**, 1
[22] Read J S, Lackey B D, Owen B J and Friedman J L 2008 *Constraints on a phenomenologically parametrized neutron-star equation of state*, *Phys. Rev.* D **79** 124032
[23] Karageorgis P and StalkerJ G 2007 *Sharp bounds on 2m/r for static spherical objects*, *Class. Quantum Grav.* **25** 195021
[24] Zloshchastiev K G 1999 *Barotropic thin shells with linear EOS as models of stars and circumstellar shells in general relativity*, Int. J. Mod. Phys. D **8**, 549
[25] Buchdahl H A 1959 *General relativistic fluid spheres*, *Phys. Rev.* **116** 1027
[26] Lobo F S N 2006 *Stable dark energy stars*, *Class. Quantum Grav.* **23** 1525
[27] Nakao K, Ida D and Sugiura N 1999 *Crossing of spherical massive shells in vacuum space-time*, Progress of Theoretical Physics **101**, 47